J. Microbiol. Biotechnol. (2013), **23**(1), 7–14
http://dx.doi.org/10.4014/jmb.1205.05062
First published online November 28, 2012
pISSN 1017-7825 eISSN 1738-8872

JOURNAL OF MICROBIOLOGY AND BIOTECHNOLOGY

Role of the Salt Bridge Between Arg176 and Glu126 in the Thermal Stability of the *Bacillus amyloliquefaciens* α-Amylase (BAA)

Zonouzi, Roseata[1]*, Khosro Khajeh[2], Majid Monajjemi[3], and Naser Ghaemi[4]

[1]*Department of Biology, Science and Research Branch, Islamic Azad University, Tehran, Iran*
[2]*Department of Biochemistry, Faculty of Biological Sciences, Tarbiat Modares University, Tehran, Iran*
[3]*Department of Chemistry, Science and Research Branch, Islamic Azad University, Tehran, Iran*
[4]*Department of Biotechnology, University College of Science, University of Tehran, Tehran, Iran*

Received: May 31, 2012 / Revised: August 25, 2012 / Accepted: August 29, 2012

In the *Bacillus amyloliquefaciens* α-amylase (BAA), the loop (residues 176–185; region I) that is the part of the calcium-binding site (CaI, II) has two more amino acid residues than the α-amylase from *Bacillus licheniformis* (BLA). Arg176 in this region makes an ionic interaction with Glu126 from region II (residues 118–130), but this interaction is lost in BLA owing to substitution of R176Q and E126V. The goal of the present work was to quantitatively estimate the effect of ionic interaction on the overall stability of the enzyme. To clarify the functional and structural significance of the corresponding salt bridge, Glu126 was deleted (ΔE126) and converted to Val (E126V), Asp (E126D), and Lys (E126K) by site-directed mutagenesis. Kinetic constants, thermodynamic parameters, and structural changes were examined for the wild-type and mutated forms using UV-visible, atomic absoption, and fluorescence emission spectroscopy. Wild-type exhibited higher k_{cat} and K_m but lower catalytic efficiency than the mutant enzymes. A decreased thermostability and an increased flexibility were also found in all of the mutant enzymes when compared with the wild-type. Additionally, the calcium content of the wild-type was more than ΔE126. Thus, it may be suggested that ionic interaction could decrease the mobility of the discussed region, prevent the diffusion of cations, and improve the thermostability of the whole enzyme. Based on these observations, the contribution of loop destabilization may be compensated by the formation of a salt bridge that has been used as an evolutionary mechanism or structural adaptation by the mesophilic enzyme.

Key words: *Bacillus amyloliquefaciens* α-amylase, ionic interaction, site-directed mutagenesis, thermal stability

*Corresponding author
Phone: +98-21-44865939; Fax: +98-21-44865767;
E-mail: Roseata_Zonouzi@yahoo.com

Bacterial α-amylases provide useful materials for research on the relationship between the protein amino acid sequence and the stability of its biologically active conformation, which is one of the central problems of molecular biology [33]. The α-amylases from *B. amyloliquefaciens* (BAA), *B. stearothermophilus* (BStA), *B. licheniformis* (BLA), and *Bacillus* sp. strain KSM-1378 (AmyK) are liquefying-type enzymes, and their primary structures resemble one another. When suitably aligned, the deduced amino acid sequence of BAA exhibits 80%, 66%, and 66.7% identities to those of BLA [42], BStA [32], and AmyK [35], respectively. Despite the resemblance of their primary structures, they show diversity in heat and pH stabilities; the thermal stability dramatically increases in the following order *Bacillus* sp. strain KSM-1378 [16], *B. amyloliquefaciens, B. stearothermophilus,* and *B. licheniformis* [38]. The three-dimentional structures of BLA [22], BStA [32], AmyK [29], BAA [1], and other *Bacillus* amylases have been determined. All the X-ray structures of α-amylases reported so far contain a calcium ion with high affinity at a conserved calcium-binding site, which is located at the interface between domains A and B (CaI) [3, 21, 22]. CaI connects domains A to B and, therefore, contributes to stabilization of the active site structure and controls the formation of the extended substrate-binding site [22]. The second calcium ion (CaII) is located close to the conserved calcium ion (CaI), and in the presence of a sodium ion, they form a calcium-sodium-calcium metal triad at the interface of domains A and B. This triadic array exists in *B. licheniformis* α-amylase (BLA) [22] and that from closely related *Bacillus* species such as α-amylase from *B. amyloliquefaciens* (BAA) [4] and *B. stearothermophilus* (BStA) [32]. It is the common feature of α-amylases that calcium ion is required for their structural integrity, thermal stability, as well as enzymatic activity [24, 39]. Domain B has a significant contribution in the total flexibility

of BAA [1], and residues 176–185 (region I or loop) from this domain construct part of the cage responsible for attachment to the calcium [9, 21, 22]. Suzuki *et al.* [33] demonstrated that thermostability of BAA was drastically improved by deletion of Arg176-Gly177 and substitution of Lys269Ala using site-directed mutagenesis. They proposed that an increase in hydrophobicity enhanced the thermostability of the enzyme. Machius *et al.* [21, 22] also suggested that the loop containing Arg-Gly residues in BAA has two more amino acid residues than BLA that could cause an increase in mobility of this region and decrease the thermostability of the whole protein. The bulge that was created in this region [1] could facilitate the loop displacement and cation diffusion when the temperature rises. On the other hand, the first flexible region of BLA, residues 118–130 (region II), is more flexible and accessible than BAA [17]. Arg176 from region I makes an ionic interaction with Glu126 (from region II) (Fig. 1), but this interaction is lost in BLA owing to substitution of R176Q and E126V, so the corresponding loop in BLA has plunged into the structure instead of interacting to the distal part of the structure [1]. Therefore, it might be speculated that (i) deletion of Glu126 would produce conformational release, leading to thermostability by compactness of the BAA structure [1], and (ii) the contribution of loop stabilization by shortening two amino acid residues to the thermostabilization of BLA may be compensated by the corresponding salt bridge in BAA, so the presence of this interaction may cause a decrease in the flexibility and, therefore, increase the conformational stability of the enzyme.

To examine which prediction is actually applicable to BAA, Glu126 was deleted (ΔE126) and changed to Val (E126V), Asp (E126D), and Lys (E126K) by site-directed mutagenesis. The mutants were used as valuable materials for structural studies, such as UV-visible, atomic absoption, and fluorescence emission spectroscopy. Structural changes during the thermoinactivation process were monitored and compared with the wild-type.

A

BAA	**117**	E V N P A N R N Q **E** T S E E Y	**171** R I F K F R G **E G** K A W
BLA	**119**	E V D P A D R N R **V** I S G E H	**172** R I Y K F Q G - - K A W
BStA	**120**	E V N P S D R N Q **E** I S G T Y	**174** R I Y K F R G **I G** K A W
AmyK	**121**	E V N R S N R N Q **E** I S G E Y	**176** K I Y K F R G **T G** K A W

B

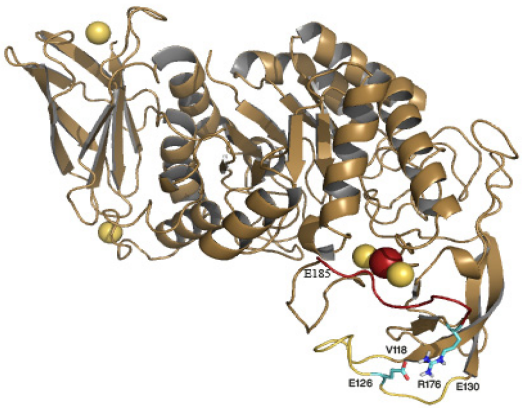

Fig. 1. (**A**) Amino acid sequence alignment of the selected α-amylases surrounding Glu126 and Arg176 of BAA (PDB code 3BH4), BLA (PDB code 1BLI), BStA (PDB code 1HVX), and AmyK (PDB code 2DIE), and (**B**) the BAA structure was illustrated on the basis of the crystal structure of *Bacillus amyloliquefaciens* α-amylase (BAA) (PDB code 3BH4) by Pymol 0.99 rc6.
Region I (residues E185–R176) and II (residues V118–E130) are represented by red and yellow colors, and calcium and sodium ions are presented by yellow and red color spheres, respectively. The existing salt bridge is between residues R176 (from region I) and E126 (from region II).

Materials and Methods

Materials

All chemicals used were of reagent grade or higher. Oligonucleotides were synthesized by MWG (Germany). The genomic DNA extraction kit was obtained from Real Biotech. (Taiwan). PWO (DNA polymerases from *Pyrococcus woesei*) was purchased from Roche (Germany). The restriction enzymes, T4 ligase, DpnI, IPTG (isopropyl-ß-D-1-thiogalactopyranoside), and PCR reagents were supplied by Fermentas (Germany). 3,5-Dinitrosalicylic acid (DNS) and Tris were purchased from Sigma (USA). The Ni-NTA agarose was obtained from Amersham Biosciences (USA), and pET21a vector was from Novagen (USA). *Escherichia coli* XL1 Blue and *E. coli* BL21 (DE3) were obtained from Stratagene (USA). All other chemicals were from Merck (Germany).

Bacterials Strains, Plasmid, and Growth Conditions

Bacillus amyloliquefaciens (ATCC 23350), isolated from soil samples, was obtained from the Iranian Centre of Industrial Fungi and Bacteria Collection. *Escherichia coli* XL1 Blue and *E. coli* BL21 (DE3) were used as hosts for cloning and expression, respectively. The PCR product was cloned into the expression vector pET21a (+). *Bacillus amyloliquefaciens* was cultured in medium containing (g/l) peptone (5), meat extract (3), agar (15), and $MnSO_4 \cdot H_2O$ (0.01) at 30°C. *Escherichia coli* strains were grown overnight in Luria–Bertani (LB) medium [27] at 37°C.

Cloning of the BAA Gene in pET21a

The genomic DNA was isolated from BAA using a genomic DNA extraction kit. Primers were made by removing the coding sequence for the signal peptide and introducing *Nde*I and *Not*I restriction sites at the 5' and 3' ends, respectively:
5'-GGAATTCCATATGGTAAACGGTACGCTGATGCAG-3' (forward) and 5'-ATAAGAATGCGGCCGCTTTCTGAACATAAATGGAGA CGG-3' (reverse). The α-amylase gene was amplified from purified total DNA using the polymerase chain reaction (PCR). The PCR product was digested with *Nde*I and *Not*I restriction enzymes and ligated into the restriction enzymes-cleaved pET21a (+) with T4 DNA ligase at 37°C for 12 h [15]. Then the ligation mixture was transformed into *E. coli* XL1 Blue [6]. Sequencing was performed using an automatic sequencer (MWG, Germany) by the T7 promoter and T7 terminator universal primers.

Site-Directed Mutagenesis

Mutagenesis was carried out using the QuikChange site-directed mutagenesis method described by Fisher and Pei [12]. Then two pairs of chemically synthesized oligonucleotides (MWG, Germany) were designed as follows:

Glu126Val forward: 5'-CCAATAGAAATCAGGTGACTTCGGAGG AATATC-3'

Glu126Val reverse: 5'-GATATTCCTCCGAAGTCACCTGATTTCTAT TGG-3'

Glu126Asp forward: 5'-GCCAATAGAAATCAGGATACTTCGGAG GAATATC-3'

Glu126Asp reverse: 5'-GATATTCCTCCGAAGTATCCTGATTTC TATTGGC-3'

Glu126Lys forward: 5'-GGCCAATAGAAATCAGAAAACTTCGGA GGAATATC-3'

Glu126Lys reverse: 5'-GATATTCCTCCGAAGTTTTCTGATTTC TATTGGCC-3'

ΔGlu126 forward: 5'-GGCCAATAGAAATCAG|ACTTCGGAGGA ATATC-3'

ΔGlu126 reverse: 5'-GATATTCCTCCGAAGT|CTGATTTCTATTGG CC-3'

The 50 μl PCR mixture contained 0.2 μg of template DNA, 10× PCR buffer, 15 μM of each primer, 0.2 mM of each dNTP, and PWO polymerase (1.25 units). The mixture was heated at 95°C for 5 min and then subjected to thermal cycling (22 cycles of 95°C for 1 min, 55°C for 1 min, and 68°C for 13 min). The PCR product was incubated with DpnI at 37°C for 2 h to digest parental DNA template. The remaining product was transformed into *E. coli* XL1-blue by the chemical transformation method [6]. Five clones were selected randomly for sequencing and the mutagenesis was confirmed by MWG Germany.

Protein Expression and Purification

The constructed expression plasmid was used to transform *E. coli* strain BL21 (DE3). Transformants carrying BAA genes were grown at 37°C for overnight in 10 ml of Luria–Bertani medium supplemented with ampicillin (100 mg/ml). Subsequently, 300 ml of medium was inoculated with 500 μl of overnight culture and grown at 37°C with vigorous shaking until the OD_{600} reached 0.6, after which IPTG was added to a final concentration of 1.5 mM and the culture was further incubated (overnight) at 22°C with vigorous shaking. The cells were harvested by centrifugation (5,000 ×*g* for 15 min) and lyzed by sonication in buffer containing 50 mM Tris-HCl and 50 mM NaCl (pH 7.5). The pellet was then harvested by centrifugation (6,000 ×*g*, 15 min) and incubated in lysis buffer (50 mM Tris-HCl, 300 mM NaCl, 6 M urea, pH 7.5) for 2 h at room temperature and refolded by sequential dialysis against 4, 3, 2, 1, and 0 M urea in 50 mM Tris-HCl (pH 7.5), 50 mM NaCl, and 1 mM dithiothreitol. The cells were removed by centrifugation (10,000 ×*g*) for 20 min at 4°C and the supernatant was used for further purification. Purification was carried out using an Ni-NTA agarose column as described by the manufacturer (Amersham Biosciences).

Determination of the Enzymatic Activity and Protein Concentration

α-Amylase was assayed at room temperature using potato starch as a substrate in 50 mM Tris buffer (pH 7.5) containing 50 mM NaCl and 10 mM $CaCl_2$. The concentration of reducing sugars obtained from the catalyzed reaction was measured by the dinitrosalicylic acid method according to Bernfeld [2]. Protein concentration was determined by the Lowry method [20]. In order to determine the kinetic parameters, measurements were carried out using 15 different substrate concentrations ranging from 0.2 to 10 K_m. We had blanks for each starch concentration and the differential absorbance was used to determine the activity. Initial velocities data were fitted to the Michaelis–Menten equation, and steady-state kinetic parameters K_m, V_{max}, k_{cat} and k_{cat}/K_m for mutants and the wild-type were determined [11]. The results are the mean value of three independent experiments that were repeated for reproducibility.

Measurements of Thermal Inactivation, and Optimum pH and Temperature of the Enzymes

Purified BAA and mutants in 50 mM Tris-HCl, 50 mM NaCl, 10 mM $CaCl_2$, pH 7.5 were incubated at 75°C and 80°C for differing times, and samples were snap-cooled in an ice-water bath and then assayed for residual activity at 37°C. Plots of the log of residual activity versus time were linear, indicating a first-order decay process under these conditions, where the slope gave the value of the inactivation rate constant k_{inact} [14].

The specific activity of the wild-type and mutant enzymes were measured at various pHs after 30 min at given temperatures (10°C to 80°C) for the mutant and wild-type enzymes. The buffers used (50 mM) were as follows: Glycine-HCl buffer (pH 2.2–3.6), Sodium acetate buffer (pH 3.6–5.6), Phosphate buffer (pH 5.6–8.6), and Glycine-NaOH buffer (pH 8.6–10.6).

Calculation of Thermodynamic Parameters

The apparent first-order rate constants (k_{cat}, k_{inact}) were used to calculate the energy of activation according to the Arrhenius equation:

$$k = A\, e^{-Ea/RT}$$

where k (s^{-1}) is the rate constant at temperature T (K), A is a pre-exponential factor related to steric effects and the molecular collision frequency, R is the gas constant (8.314 J mol^{-1} K^{-1}), and E_a is the activation energy of the reaction. Hence, a plot of ln k versus 1/T gives a straight line with the slope being $-E_a/R$. The thermodynamic parameters of activation were determined as follows:

$$\Delta G^{\#} = RT\ \ln(k_B T/h) - RT\ln k$$

$$\Delta H^{\#} = E_a - RT$$

$$\Delta S^{\#} = \frac{\Delta H^{\#} - \Delta G^{\#}}{T}$$

where k_B is the Boltzmann constant (1.3805×10^{-23} J K^{-1}), h is Planck's constant (6.6256×10^{-34} J s), k (s^{-1}) is the rate constant at temperature T (K), $\Delta G^{\#}$ is the energy barrier for the reaction, $\Delta H^{\#}$ is the activation enthalpy, and $\Delta S^{\#}$ is the activation entropy. All measurements were performed in at least three independent experiments. The deviations from the averages that are shown in this study were less than 10%.

Fluorescence Quenching by Acrylamide

Measurements were carried out in a protein solution (final concentration 50 μg/ml) with different acrylamide concentrations ranging from 0 to 0.3 M, using acrylamide stock (2 M) at 25°C. Emission spectra were recorded between 300 and 400 nm at an excitation wavelength of 280 nm. Quenching data were analyzed in terms of the Stern–Volmer constant, K_{SV}, which was calculated from the ratio of the

unquenched and the quenched fluorescence intensities, F0/F, using the relationship $F0/F = 1 + K_{SV}[Q]$. Q is the molar concentration of the quencher [10]. The intrinsic protein fluorescence F was corrected for the acrylamide inner filter effect f, the latter being defined as shown in the following equation:

$$f = 10^{-\varepsilon[Q]/2}$$

using an extinction coefficient of 4.3 M^{-1} cm^{-1} for acrylamide at 280 nm.

Determination of Calcium Content

The purified enzymes were dialyzed at 5°C against 20 mM Tris-HCl (pH 7.5). Quantitative determination of the calcium content of wild-type BAA and ΔGlu126 were performed by atomic absorption spectrophotometry in three runs, each in triplicate. The system was calibrated using metal calibration standard solutions in the range of 0–5 ppm. The buffer was also used as a control and its value was subtracted from the sample values. These data allowed us to calculate the mole of calcium per mole of enzyme.

Results and Discussion

Influence of the Mutations on the Kinetic Constants

The kinetic parameters k_{cat} and K_m were determined for the wild-type and mutant enzymes. All mutants exhibited lower k_{cat} and K_m but higher catalytic efficiency than the wild-type (Table 1). The catalytic efficiency of the wild-type was less than other known mutants. These results indicate that the substitution and deletion not only abolished the amylase activity but also significantly affected the catalytic efficiency of the enzymes. As previously reported, amino acids implicated in the catalytic reaction of α-amylase has generally been localized in four highly conserved regions [23]. Since Glu126 of BAA is not situated in these regions, mutations improved catalytic efficiency through decreasing K_m, not increasing k_{cat}. The specific activities of the four recombinant enzymes were measured at different pH values. The optimum pH for the enzymes was around 6.5–7.

In order to understand the decrease in k_{cat}, the temperature dependence of the catalytic activity and structural changes of the variants during the thermoinactivation process were studied.

Temperature Dependence of the Catalytic Activity

In various studies, the activity of several α-amylases was measured as a function of temperature. One use of these measurements was to determine the optimum temperature for maximal enzyme activity, which is an important parameter in characterizing the thermal adaptation process [7, 13]. The T_{opt} could be related to the thermostabilities of the selected α-amylases. Unexpectedly, in the presence of 10 mM $CaCl_2$, all of the mutant α-amylases showed a temperature optimum as low as that of BAA (55°C). To clarify the specific role of Glu126, which is reflected in a lower k_{cat}, the activities of E126V, E126D, E126K, and ΔE126 as a function of temperature were analyzed. Based on thermodynamic calculations at 55°C, all mutants exhibited higher $\Delta G^{\#}$ but lower activation energy (E_a), activation enthalpy ($\Delta H^{\#}$), and activation entropy ($\Delta S^{\#}$) than the wild-type (Table 2). As expected, the activation free energy barrier ($\Delta G^{\#}$) obtained for the mutant enzymes was greater than the wild-type, because of the negative effects of the activation entropy ($\Delta S^{\#}$) and positive effects of the activation enthalpy. Thus the removal of the salt bridge decreased the activation entropy, suggesting an increase in the local flexibility at the loop relative to the wild-type. According to recent studies, the introduction or removing of the salt bridge in the mesophilic or the thermophilic enzyme changed the activation energy, which was accompanied by changes in both activation enthalpy and entropy [19].

Thermal Inactivation

The thermal denaturation of enzymes is accompanied by the disruption of noncovalent linkages, including hydrophobic interactions, with concomitant increase in the enthalpy of activation [8]. The opening up of the enzyme structure is accompanied by an increase in the disorder, randomness, or entropy of activation [41]. In order to understand the effects of the corresponding salt bridge in the protein structure, thermoinactivation rates for all variants were determined at 75°C and 80°C in the presence of 10 mM $CaCl_2$ (Fig. 2). Irreversible thermoinactivation of the wild-type and its variant was also compared. As shown in Table 2, the wild-type (BAA) had a half-life of 167 and 45 min at 75°C and 80°C, respectively. All the

Table 1. Kinetic constants of wild-type and mutant BAAs.

Enzymes	Kinetic parameters			Optimum pH
	K_m ($\times 10^3$ μM)	k_{cat} (s^{-1})	k_{cat}/K_m ($\times 10^{-3}$ μM^{-1} s^{-1})	
Wild-type	16.9 ± 1.45	186.6 ± 4	11.04 ± 0.01	6.5–7
E126V	13.1 ± 0.29	183.4 ± 2	14.00 ± 0.10	6.5–7
E126D	13.4 ± 0.29	181.4 ± 2	13.54 ± 0.10	6.5–7
E126K	11.1 ± 0.58	142.6 ± 5	12.85 ± 0.05	6.5–7
ΔE126	11.7 ± 0.58	129.4 ± 6	11.06 ± 0.01	6.5–7

Kinetic parameters were measured from initial rates at different concentrations of starch over the range 0.2 to 10 K_m, at 37°C in 50 mM Tris buffer (pH 7.5) containing 50 mM NaCl and 10 mM $CaCl_2$.

Table 2. Thermodynamic parameters and structural parameter of wild-type and mutant BAAs.

Enzymes	T_{opt}[a] (°C)	Half-lives[b] (min) at (°C)		Activation[b] (kcal/mol)				Inactivation[b] (kcal/mol)				K_{sv}[b]
		75	80	E_a	$\Delta H^{\#}$	$\Delta G^{\#}$	$T\Delta S^{\#}$	E_a	$\Delta H^{\#}$	$\Delta G^{\#}$	$T\Delta S^{\#}$	(M^{-1})
Wild-type	55	167 ± 2	45 ± 1	9.3 ± 0.2	8.6 ± 0.2	15.8 ± 0.1	-7.2 ± 0.1	63.0 ± 2	62.3 ± 2	24.9 ± 0.1	37.4 ± 2	11.4 ± 1
E126V	55	155 ± 2	26 ± 2	7.5 ± 0.4	8.9 ± 0.4	15.9 ± 0.1	-9.0 ± 0.3	57.4 ± 1	56.7 ± 1	24.6 ± 0.2	32.1 ± 1	13.7 ± 0.5
E126D	55	94 ± 1	24 ± 2	6.0 ± 0.3	5.3 ± 0.3	15.9 ± 0.1	-10.6 ± 0.2	57.0 ± 1	56.3 ± 1	24.4 ± 0.2	31.9 ± 1	15.0 ± 1
E126K	55	46 ± 1	11 ± 1	5.1 ± 0.3	4.5 ± 0.3	16.0 ± 0.1	-11.6 ± 0.2	39.2 ± 3	38.5 ± 3	23.9 ± 0.1	14.6 ± 3	16.5 ± 1
ΔE126	55	2 ± 0.2	1.2 ± 0.1	4.3 ± 0.5	3.6 ± 0.5	16.1 ± 0.1	-12.5 ± 0.4	26.7 ± 2	26.0 ± 2	22.4 ± 0.3	3.60 ± 2	17.3 ± 0.5

T_{opt} was calculated at the given temperatures (10°C to 80°C), and half-lives ($t_{1/2}$) of thermoinactivations were obtained for mutants and wild-type enzymes in the presence of 10 mM $CaCl_2$. The thermodynamic parameters of activation were determined at 55°C. Thermodynamic parameters for irreversible thermoinactivation of activity ($k_{inactivation}$) were calculated at 75°C. Fluorescence quenching was carried out by the addition of 2 M acrylamide to protein solutions (50 μg/ml) at an excitation wavelength of 280 nm.

[a]Values are the averages of three experiments and standard errors are less than 10%.

[b]Values are the averages of three experiments.

mutant enzymes were more sensitive to heat inactivation than the wild-type. Among the mutants, ΔE126 showed a notable decrease in the thermoresistance of enzyme, whereas the other variants led to slower inactivation rates and more prolonged half-lives. Differences in half-lives among E126V, E126D, E126K, and the wild-type diminished at higher temperatures, due to the fact that irreversible inactivation is increased at elevated temperatures as a result of increased structural flexibility. The calcium ion binding affects the inactivation properties and thermodynamic parameters of BAA and some enzymes [18, 36]. Results indicate that the thermal stability of mutants and wild-type enzyme are strongly dependent on calcium ion (data not shown), as reported before in wild-type [26]. Thus, the calcium content of wild-type BAA and ΔE126 was determined by atomic absorption spectrophotometry. Values of 3.7±0.2 and 1.8±0.4 (mole/mole; Ca^{2+}/enzyme) were obtained for wild-type BAA and ΔE126, respectively. Analysis of the thermodynamic parameters of activation for the inactivation process (Table 2) at 75°C showed that, as expected, the inactivation rate constant (k_{inact}) for wild-type was the lowest and, correspondingly, the energy barrier for inactivation $\Delta G^{\#}$ was the highest. Moreover, the positive apparent activation entropy was higher in the wild-type and was compensated by a higher activation enthalpy. The irreversible inactivation of BAA was explained by a simple two-step mechanism: calcium ion depletion, followed by an irreversible conformational change [36]. Therefore, our calculated parameters may consist of the contributions of both calcium-binding and irreversible thermoinactivation of the enzyme. Indeed, weakening of the calcium-binding may be the reason for the decreased thermodynamic parameters of all mutants.

The activation entropy represents the difference in the extent of local disordering between the transition state and the ground state for the inactivation pathway. Thus, the positive $\Delta S^{\#}$ is in agreement with increasing local disorder in the transition state when compared with the ground state [5, 30]. The increasing $\Delta S^{\#}$ value as a function of calcium concentration is considered to be due to the degree of disorder in the structure needed to reach the transition state for the unfolding, because the structural packing in the ground state was firmly stabilized by the calcium ion. Therefore, the corresponding salt bridge between Arg176 and Glu126 might be entropically favorable at high temperatures via restricting flexibility.

Fluorescence Quenching by Acrylamide

The results of quenching experiments allow us to assess the relative solvent exposure of different types of fluorophores. The more exposed a fluorophore is, the more effective the collisional quencher will be in reducing the fluorescence intensity displayed by that molecule [7, 10, 40]. Fig. 3 depicts the Stern–Volmer plot and fluorescence quenching by acrylamide at pH 7.5. The quenching constants (K_{SV} values) calculated for the wild-type was lower than for the mutants (Table 2). The Stern–Volmer plot indicates that the aromatic amino acids in mutants are more exposed compared with the wild-type; therefore, tryptophan fluorescence is quenched more in the case of the former. Therefore, this result indicates more solvent exposed Trp residues in the mutants. On the other hand, mutation induces a looser and more flexible environment around the aromatic residues.

Natural deletions in the BLA loop (region I) have created a favorable backbone strain that is nearly parallel with the corresponding salt bridge in BAA and is responsible for decreasing the displacement and flexibility of the loop and diffusion of cations. It has been suggested that the structure in BAA is stabilized by this interaction. First, the destabilizing effect of the loop length has been rationalized theoretically by the increase in the entropic

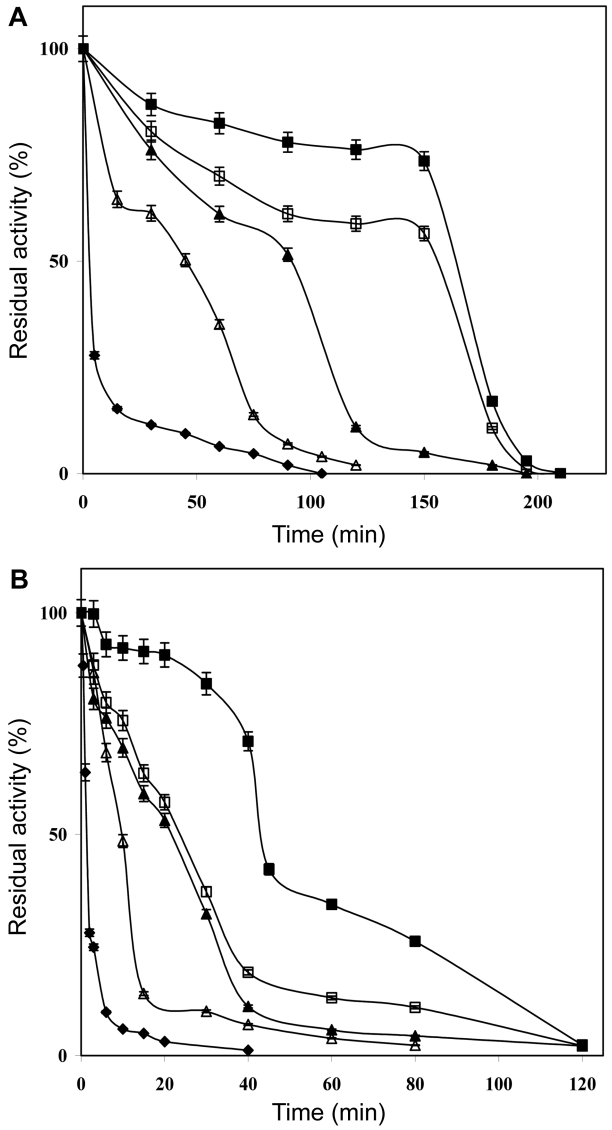

Fig. 2. Thermoinactivation of wild-type BAA (■) and its mutants E126V(□), E126D(▲), E126K(△), and ΔE126(◆) in 50 mM Tris-HCl, 50 mM NaCl, pH 7.5, at different temperatures in the presence of 10 mM $CaCl_2$; (**A**) 75°C and (**B**) 80°C.
Standard deviations were within 5% of the experimental values.

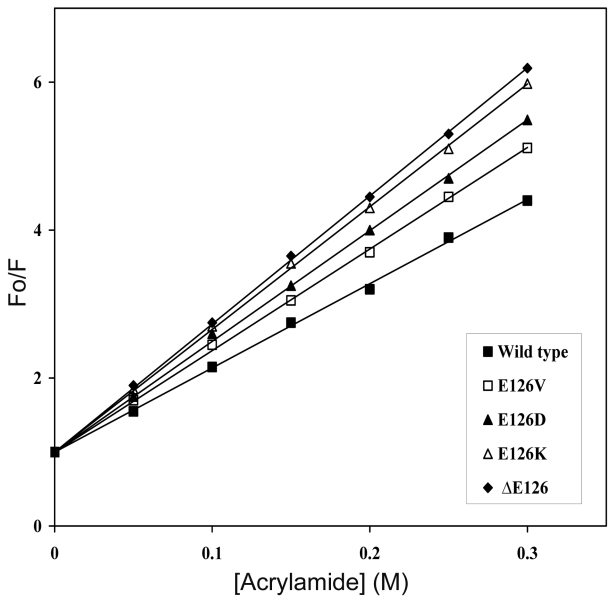

Fig. 3. Stern–Volmer plot of fluorescence quenching by acrylamide.
Fluorescence quenching at 25°C for wild-type and mutant BAAs at pH 7.5.

cost of forming a loop. Second, this interaction decreases the movement of the flexible loop and region II. Therefore, the corresponding salt bridge in the wild-type might be responsible for the decrease in the entropy changes by reducing the amount of water molecules around regions I and II through increasing internal packing. Thus, deletion of this interaction expands the cavity to be formed between the two regions (I, II) and exposes the calcium-binding site to water and calcium diffusion. According to computational modeling of the mutants, the notable change in flexibility upon the removal of the salt bridge was localized in the side-chain conformation of the loop arginine residue, because the unrestrained arginine residue can populate more rotamer conformations and is directed toward the surface.

In conclusion, we have shown that the deletion and substitution of Glu126, which is located in a loop within domain B of BAA, decreased thermostability and increased flexibility. The difference in the stability of α-amylases from *B. amyloliquefaciens* (BAA) and *B. licheniformis* (BLA) was due to differences in the degree of internal packing. Loosening of the internal packing might be responsible for the increase in the amount of water molecules around the enzymes and thus the increase in the entropy changes of both α-amylases [33]. Sequence analyses revealed that shortening of exposed loop regions has been used by thermophilic organisms as an evolutionary mechanism to create more thermally stable enzymes [37], like BLA. Based on our studies, the bulge created in the loop region could facilitate the loop displacement [1], and ionic interaction between Arg176 (region I) and Glu126 (region II) adds to the overall stability of the surface loop through decreasing loop flexibility and preventing diffusion of cations when the temperature rises. Therefore, in BAA, the contribution of loop destabilization by inserting two amino acid residues may be compensated by the corresponding salt bridge, which has been used as an evolutionary mechanism by the mesophilic enzymes. Indeed, the salt bridge is a structural adaptation for mesophilic α-amylase. However, further study will be required to more thoroughly elucidate the microenvironmental topology around the two discussed regions (I, II) in the BAA thermostability.

REFERENCES

1. Alikhajeh, J., K. Khajeh, B. Ranjbar, H. Naderi-Manesh, Y. H. Lin, E. Liu, *et al*. 2010. The crystal structure of *Bacillus amyloliquefaciens* α-amylase at high resolution: Implications for thermal stability. *Acta Crystallogr. Sect. F. Struct. Biol. Cryst. Commun*. **66:** 121–129.
2. Bernfeld, P. 1955. Amylase, α and β. *Methods Enzymol*. **1:** 149–151.
3. Boel, E., L. Brady, A. M. Brzozowski, Z. Derewenda, G. G. Dodson, V. J. Jensen, *et al*. 1990. Calcium-binding in α-amylases: An X-ray diffraction study at 2.1 Å resolution of two enzymes from *Aspergillus*. *Biochemistry* **29:** 6244–6249.
4. Brzozowski, A. M., D. M. Lawson, J. P. Turkenburg, H. Bisgaard-Frantzen, A. Svendsen, T. V. Borchert, *et al*. 2000. Structural analysis of a chimeric bacterial α-amylase: High-resolution analysis of native and ligand complexes. *Biochemistry* **39:** 9099–9107.
5. Chen, X. and C. R. Matthews. 1994. Thermodynamic properties of the transition state for the rate-limiting step in the folding of the α-subunit of tryptophan synthase. *Biochemistry* **33:** 6356–6362.
6. Chung, C. Y., S. L. Niemela, and R. H. Miller. 1989. One-step preparation of competent *Escherichia coli* : Transformation and storage of bacterial cells in the same solution. *Proc. Natl. Acad. Sci. USA* **86:** 2172–2175.
7. D'Amico, S., J. C. Marx, C. Gerdy, and G. Feller. 2003. Activity stability relationships in extremophilic enzymes. *J. Biol. Chem*. **278:** 7891–7896.
8. Daniel, R. M. 1996. The upper limits of enzyme thermal stability. *Enzyme. Microb. Technol*. **19:** 74–79.
9. Declerck, N., M. Machius, G. Wiegand, R. Huber, and C. Gaillardin. 2000. Probing structural determinants specifying high thermostability in *Bacillus licheniformis* alpha-amylase. *J. Mol. Biol*. **301:** 1041–1057.
10. Eftink, M. R. and C. A. Ghiron. 1976. Exposure of tryptophanyl residues and protein dynamics. *Biochemistry* **16:** 5546–5551.
11. Fersht, A. 1999. *Structure and Mechanism in Protein Science*. W. H. Freeman and Co., New York.
12. Fisher, C. L. and G. K. Pei. 1997. Modification of a PCR-based site-directed mutagenesis method. *BioTechniques* **23:** 570–574.
13. Fitter, J., R. Herrmann, N. A. Dencher, A. Blume, and T. Hauss. 2001. Activity and stability of a thermostable α-amylase compared to its mesophilic homologue: Mechanism of thermal adaptation. *Biochemistry* **40:** 10723–10731.
14. Gouda, M. D., S. A. Singh, A. G. A. Rao, M. S. Thakur, and N. G. Karanth. 2003. Thermal inactivation of glucose oxidase. *J. Biol. Chem*. **278:** 24324–24333.
15. Haghani, K., Kh. Khajeh, H. Naderi-Manesh, and B. Ranjbar. 2012. Evidence regarding the hypothesis that the histidine-histidine contact pairs may affect protein stability. *Int. J. Biol. Macromol*. **50:** 1040–1047.
16. Igarashi, K., H. Hagihara, and S. Ito. 2003. Protein engineering of detergent α-amylases. *Trends Glycosci. Glycotechnol*. **82:** 101–114.
17. Khajeh, Kh., M. M. Shokri, S. M. Asghari, F. Moradian, A. Ghasemi, M. Sadeghi, *et al*. 2006. Acidic and proteolytic digestion of α-amylases from *Bacillus licheniformis* and *Bacillus amyloliquefaciens*: Stability and flexibility analysis. *Enzyme Microb. Technol*. **38:** 422–428.
18. Kuroki, R., S. Kawakita, H. Nakamura, and K. Yutani. 1992. Entropic stabilization of a mutant human lysozyme induced by calcium-binding. *Proc. Natl. Acad. Sci.USA* **89:** 6803–6807.
19. Lam, S. Y., R. C. Y. Yeung, T. Yu, K. Sze, and K. Wong. 2011. A rigidifying salt-bridge favors the activity of thermophilic enzyme at high temperatures at the expense of low-temperature activity. *PLoS Biol*. **9:** e1001027.
20. Lowry, O. H., N. J. Rosebrough, A. L. Farr, and R. J. Randall. 1951. Protein measurement with folin phenol reagent. *J. Biol. Chem*. **193:** 265–275.
21. Machius, M., G. Wiegand, and R. Huber. 1995. Crystal structure of calcium depleted *Bacillus licheniformis* α-amylase at 2.2 Å resolution. *J. Mol. Biol*. **246:** 545–559.
22. Machius, M., N. Declerck, R. Huber, and G. Wiegand. 1998. Activation of *Bacillus licheniformis* alpha-amylase through a disorder → order transition of the substrate-binding site mediated by a calcium-sodium-calcium metal triad. *Structure* **6:** 281–292.
23. Matsuura, Y., M. Kusunoki, W. Harada, and M. Kakudo. 1984. Structure and possible catalytic residues of Taka-amylase A. *J. Biochem. (Tokyo)* **95:** 699–702.
24. Nielsen, J. E. and T. V. Borchert. 2000. Protein engineering of bacterial α-amylases. *Biochim. Biophys. Acta.* **1543:** 253–274.
25. Protasevich, I., B. Ranjbar, V. Lobachov, A. Makarov, R. Gilli, C. Briand, *et al*. 1997. Conformation and thermal denaturation of apocalmodulin: Role of electrostatic mutations. *Biochemistry* **36:** 2017–2024.
26. Saboury, A. A. and F. Karbassi. 2000. Thermodynamic studies on the interaction of calcium ions with alpha-amylase. *Thermochim. Acta.* **362:** 121–129.
27. Sambrook, J., E. F. Fritsch, and T. Maniatis. 1989. *Molecular Cloning: A Laboratory Manual*. Cold Spring Harbor Laboratory Press, Cold Spring Harbor, New York.
28. Schippers, P. H. and H. P. J. M. Dekkers. 1981. Direct determination of absolute circular dichroism data and calibration of commercial instrument. *Anal. Chem*. **53:** 778–788.
29. Shirai, T., K. Igarashi, T. Ozawa, H. Hagihara, T. Kobayashi, K. Ozaki, and S. Ito. 2007. Ancestral sequence evolutionary trace and crystal structure analyses of alkaline α-amylase from *Bacillus* sp. KSM-1378 to clarify the alkaline adaptation process of proteins. *Proteins* **66:** 600–610.
30. Stein, R. A. and J. V. Staros. 1996. Thermal inactivation of the protein tyrosine kinase of the epidermal growth factor receptor. *Biochemistry* **35:** 2878–2884.
31. Stryer, L. 1968. Fluorescence spectroscopy of proteins. *Science* **162:** 526–540.
32. Suvd, D., Z. Fujimoto, K. Takase, M. Matsumura, and H. Mizuno. 2001. Crystal structure of *Bacillus stearothermophilus* alpha-amylase: Possible factors determining the thermostability. *J. Biochem*. **129:** 461–468.
33. Suzuki, Y., N. Ito, T. Yuuki, H. Yamagata, and S. Udaka. 1989. Amino acid residues stabilizing a *Bacillus* alpha-amylase against irreversible thermoinactivation. *J. Biol. Chem*. **264:** 18933–18938.
34. Takakuwa, T., T. Konno, and H. A. Meguro. 1985. New standard substance for calibration of circular dichroism: Ammonium d-10-camphorsulfonate. *Anal. Sci.* **1:** 215–225.
35. Takkinen, K., R. F. Pettersson, N. Kalkkinen, I. Palva, H. Soderlund, and L. Kaariainen. 1983. Amino acid sequence of alpha-amylase from *Bacillus amyloliquefaciens* deduced from

the nucleotide sequence of the cloned gene. *J. Biol. Chem*. **258:** 1007–1013.
36. Tanaka, A. and E. Hoshino. 2002. Calcium-binding parameter of *Bacillus amyloliquefaciens* α-amylase determined by inactivation kinetics. *Biochem. J*. **364:** 635–639.
37. Thompson, M. J. and D. Eisenberg. 1999. Transproteomic evidence of a loop-deletion mechanism for enhancing protein thermostability. *J. Mol. Biol*. **290:** 595–604.
38. Tomazic, S. J. and A. M. Klibanov. 1988. Mechanisms of irreversible thermal inactivation of *Bacillus* alpha-amylases. *J. Biol. Chem*. **263:** 3086–3091.
39. Vallee, B. L., E. A. Stein, W. N. Sumerwell, and E. H. Fischer. 1959. Metal content of α-amylases of various origins. *J. Biol. Chem*. **234:** 2901–2905.
40. Varley, P. G. and R. H. Pain. 1991. Relation between stability, dynamics and enzyme activity in 3-phosphoglycerate kinases from yeast and *Thermus thermophilus*. *J. Mol. Biol.* **220:** 531–538.
41. Vieille, C. and J. G. Zeikus. 1996. Thermozymes: Identifying molecular determinants of protein structural and functional stability. *Trends Biotechnol*. **14:** 183–190.
42. Yuuki, T., T. Nomura, H. Tezuka, A. Tsuboi, H. Yamagata, N. Tsukagoshi, and S. Udaka. 1985. Complete nucleotide sequence of a gene coding for heat- and pH-stable alpha-amylase of *Bacillus licheniformis*: Comparison of the amino acid sequences of three bacterial liquefying alpha-amylases deduced from the DNA sequences. *J. Biochem*. **98:** 1147–1156.